Published in final edited form as:
Circ Res. 2010 October 15; 107(8): 1021–1031. doi:10.1161/CIRCRESAHA.110.218966.

DNA Damage Links Mitochondrial Dysfunction to Atherosclerosis and the Metabolic Syndrome

John R. Mercer, **Kian-Kai Cheng**, **Nichola Figg**, **Isabelle Gorenne**, **Melli Mahmoudi**, **Julian Griffin**, **Antonio Vidal-Puig**, **Angela Logan**, **Michael P. Murphy**, and **Martin Bennett**

Division of Cardiovascular Medicine (J.R.M., N.F., I.G., M.M., M.B.), Department of Biochemistry (K.-K.C., J.G.), and Institute of Metabolic Sciences (A.V.-P.), University of Cambridge, Addenbrooke's Hospital; and Medical Research Council Mitochondrial Biology Unit (A.L., M.P.M.), Cambridge, United Kingdom.

Abstract

Rationale—DNA damage is present in both genomic and mitochondrial DNA in atherosclerosis. However, whether DNA damage itself promotes atherosclerosis, or is simply a byproduct of the risk factors that promote atherosclerosis, is unknown.

Objective—To examine the effect of DNA damage on atherosclerosis, we studied apolipoprotein (Apo)$E^{-/-}$ mice that were haploinsufficient for the protein kinase ATM (ataxia telangiectasia mutated), which coordinates DNA repair.

Methods and Results—$ATM^{+/-}$/$ApoE^{-/-}$ mice developed accelerated atherosclerosis and multiple features of the metabolic syndrome, including hypertension, hypercholesterolemia, obesity, steatohepatitis, and glucose intolerance. Transplantation with $ATM^{+/+}$ bone marrow attenuated atherosclerosis but not the metabolic syndrome. $ATM^{+/-}$ smooth muscle cells and macrophages showed increased nuclear DNA damage and defective DNA repair signaling, growth arrest, and apoptosis. Metabolomic screening of $ATM^{+/-}$/$ApoE^{-/-}$ mouse tissues identified metabolic changes compatible with mitochondrial defects, with increased β-hydroxybutyrate but reduced lactate, reduced glucose, and alterations in multiple lipid species. $ATM^{+/-}$/$ApoE^{-/-}$ mouse tissues showed an increased frequency of a mouse mitochondrial “common” deletion equivalent and reduced mitochondrial oxidative phosphorylation.

Conclusions—We propose that failure of DNA repair generates defects in cell proliferation, apoptosis, and mitochondrial dysfunction. This in turn leads to ketosis, hyperlipidemia, and increased fat storage, promoting atherosclerosis and the metabolic syndrome. Prevention of mitochondrial dysfunction may represent a novel target in cardiovascular disease.

Keywords

atherosclerosis; mitochondria; DNA damage; metabolic syndrome

Correspondence to Prof Bennett, Division of Cardiovascular Medicine, University of Cambridge, Box 110, Addenbrooke's Hospital, Cambridge, CB2 2QQ, United Kingdom. mrb@mole.bio.cam.ac.uk.

Disclosures
None.

Europe PMC Funders Author Manuscripts

DNA damage is present both in circulating cells of patients with atherosclerosis and their plaques. For example, coronary artery disease patients have a higher leukocyte micronucleus index (a marker of genetic instability) than healthy controls, correlated with disease severity.[1,2] However, it is not known whether DNA damage directly promotes atherosclerosis, or is a byproduct of atherosclerosis risk factors, including smoking, hypercholesterolemia, diabetes, and hypertension, all of which are associated with increased levels of reactive oxygen species (ROS). ROS can be produced from intracellular oxygen radicals generated through cytosolic NADPH oxidases[3] and by leakage from the mitochondrial respiratory chain.[4] ROS induce an array of DNA adducts, including single-and double-stranded breaks (DSBs), deletions, and chromosomal translocations that promote both genomic and mitochondrial instability.[5] Both macrophages and vascular smooth muscle cells (VSMCs) in advanced human atherosclerotic plaques have increased ROS levels.[6,7]

Although DNA damage accompanies atherosclerosis, DNA damage might also promote atherosclerosis. Werner syndrome patients are predisposed to cancer and early onset of normal aging, including osteoporosis, cataracts, graying and loss of hair, diabetes mellitus, and atherosclerosis. Werner protein guards the genetic stability of the cell, playing an integral role in base excision repair and at telomere ends.[8] Critical telomere shortening following oxidative stress-induced DNA damage may also underlie the premature cellular senescence and increased apoptosis seen in VSMCs in advanced human plaques.[9] Finally, drugs used in atherosclerosis, such as HMG-CoA (3-hydroxy-3-methyl-glutarylcoenzyme A) reductase inhibitors, directly regulate repair proteins to accelerate DNA repair, reducing DNA damage and atherosclerosis in vivo.[10]

Mitochondrial (Mt)DNA is particularly vulnerable to damage, including in vascular cells,[11] in part because it lacks protective histones, and its close proximity to the inner mitochondrial membrane. Mitochondrial damage can itself lead to increased ROS production by disrupting oxidative phosphorylation,[12] and ROS can damage MtDNA, potentially creating positive feedback. MtDNA damage is frequently observed in human atherosclerosis in both circulating and vessel wall cells, particularly a specific 4977-bp “common” deletion (Δ-MtDNA[4977]) that, although often found in low abundance, is associated with mitochondrial dysfunction.[1] MtDNA damage correlates with the extent of atherosclerosis in humans and atherosclerosis-prone apolipoprotein (Apo)$E^{-/-}$ mice and precedes atherogenesis in young ApoE$^{-/-}$ mice. Indeed, ApoE$^{-/-}$ mice deficient in manganese superoxide dismutase (MnSOD), a mitochondrial anti-oxidant enzyme, show early increases in MtDNA damage and accelerated atherogenesis.[13] However, again it is not known whether MtDNA damage promotes atherosclerosis or is a secondary consequence.

The cell possesses an extensive array of proteins to sense, transduce and signal physiological responses to DNA damage, including DNA repair, transient cycle arrest, and apoptosis and senescence if damage is excessive. The ATM (ataxia telangiectasia mutated) protein is a 350-kDa phosphatidylinositol 3-kinase-related kinase required for DNA repair and maintaining genomic homeostasis. DSBs activate ATM, which phosphorylates downstream targets to effect DNA repair, including H2AX, the cycle arrest checkpoint kinases Chk-1 and -2, and the tumor suppressor gene p53. Recent studies suggest that defective ATM function promotes atherosclerosis and metabolic abnormalities, such that ATM activators decrease atherosclerosis in ApoE$^{-/-}$ mice, and improve metabolic abnormalities in ob/ob and db/db mice.[14] ATM also promotes clearance of plasma apoB-48-carrying lipoproteins, although its mechanism is unclear.[15]

ATM also regulates mitochondrial biogenesis and MtDNA content,[16] such that ATM deficiency results in defects in mitochondrial respiration.[17] In addition, although ATM is best characterized as a DNA damage response gene, recent reports have linked loss of DNA

repair enzymes to metabolic defects, which might promote atherosclerosis.[18] ATM and H2AX phosphorylation are increased in human atherosclerosis and cells derived from human plaques, in parallel with increased DNA damage.[10] However, how ATM-induced DNA damage is linked to atherosclerosis or metabolic abnormalities remains unknown. To determine whether primary defects leading to DNA damage promote atherosclerosis, we studied ATM heterozygous mice crossed with ApoE$^{-/-}$ mice. ATM homozygosity is lethal over the time needed for atherosclerosis studies, because of profound growth retardation and cancer predisposition. We find that ATM haploinsufficiency results in DNA damage in cells that comprise atherosclerotic plaques and accelerates atherosclerosis in vivo. ATM haploinsufficiency also induces multiple features of the metabolic syndrome and mitochondrial dysfunction.

Methods

An expanded Methods section is available in the Online Data Supplement at http://circres.ahajournals.org.

Primary Cultures

ATM$^{+/-}$/ApoE$^{-/-}$ and ATM$^{+/+}$/ApoE$^{-/-}$ murine VSMCs were cultured from explanted aortas and identified by immunocytochemistry for α-smooth muscle cell actin (α-SMA) and calponin.[19] Murine macrophage cultures were obtained by PBS/BSA peritoneal lavage, yielding a 95% pure F4/80 population.[20]

DNA Damage and Repair Assays

DNA damage was assessed by micronuclei formation by Hoechst staining.[21] DNA repair was assessed using DNA microelectrophoresis (comet assay) as previously described.[22] Nuclear foci were quantified using dual antibody immunofluorescence using antibodies to phospho-ATM and γ-H2AX (1:100 and 1:200 Cell Signaling, UK) as described previously.[10]

Atherosclerosis Protocols

All animal experimental procedures conformed to animal ethical committee approval and United Kingdom Home Office licensing. C57BL6/J ApoE$^{-/-}$ mice (The Jackson Laboratory, Bar Harbor, Me) were crossed with C57BL6/J ATM$^{-/-}$ mice. Bone marrow transplantation and feeding protocols were as previously described (Online Data Supplement).[19] Blood pressure was measured noninvasively using standard PPG photoplethysmography following prior familiarization.

Histological Analysis

Plaque morphometry and histological analysis for plaque composition were performed as described previously.[19]

Lipid, Glucose, and Liver Enzyme Analysis

Lipid profiles, HbA1c, blood glucose, insulin, C-peptide, and liver transaminases were assayed from whole blood or serum using commercial enzymatic assays and HPLC. For glucose and insulin tolerance testing, mice were fasted overnight, and blood glucose assayed before intraperitoneal injection of either glucose (1 g/kg) or insulin (maximum, 1.5 U/kg).

Metabolomics

Metabolomic profiling using NMR from plasma and tissues extracts was undertaken as described in the Online Data Supplement.

PCR for MtDNA Damage

PCR products were generated using primers to identify a 101 bp control product and a 251 bp product spanning the mouse equivalent of the human common 4977-bp deletion. Full details of primer sequences and semiquantitative PCR for MtDNA adducts are provided in the Online Data Supplement.

DH2 Fluorescein and Citrate Synthase Assays

2′7′-Dichlorodihydrofluorescein (Invitrogen, D-399) was coincubated with VSMCs, and relative fluorescence index was measured (excitation, 485 nm; emission, 528 nm) to determine ROS. Whole cell citrate synthase was assayed in primary VSMCs as described in the Online Data Supplement.

Time-Lapse Videomicroscopy

Time-lapse videomicroscopy was performed using an Olympus IX70 inverted microscope as described previously.[19]

Mitochondrial Extraction

$ATM^{+/-}/ApoE^{-/-}$ and $ATM^{+/+}/ApoE^{-/-}$ mouse heart and liver were extracted into ice-cold STE buffer, diced, and transferred to a Dounce homogenizer. Unbroken cells were pelleted at 1000g for 3 minutes in a Sorval SS-34 rotor using a Sorval RC5B centrifuge. Supernatants were spun at 10 000 *g* for 10 minutes and discarded. The crude mitochondrial fraction was gently resuspended with a loose plunger before centrifugation at 10 000 *g* for 10 minutes. The pellet was resuspended and aliquoted.

Western Blotting

Western blotting and antibodies are described in the Online Data Supplement.

Complex I and Citrate Synthase Activity

Complex I activity was assayed using an Aminco DW-2000 Spectrophotometer (SLM Instruments Inc, Urbana, Ill) using the NADHUbiquinone Oxidoreductase method. Citrate Synthase activity was assayed by production of Thiobis (2N) Benzoic acid (TNB) at 412 nm, as described in the Online Data Supplement.

Statistical Analysis

Student's *t* test was used for data following a Gaussian distribution and Mann–Whitney rank sum test used under nonbinominal conditions.

Results

ATM Heterozygous Mice Develop Accelerated Atherosclerosis

$ATM^{+/-}/ApoE^{-/-}$ and $ATM^{+/+}/ApoE^{-/-}$ mice were fat fed from 6 to 20 weeks of age, and atherosclerosis examined in descending aorta and aortic root, two vascular beds that show different degrees of atherosclerosis. $ATM^{+/-}$ mice showed a 1.7- and 1.6-fold increase in aortic and aortic root atherosclerosis respectively (Figure 1A and 1B; Table). We assayed plaque cell kinetics and cell types by determining VSMC and macrophage accumulation, cell death and proliferation. The percentage areas occupied by VSMCs or macrophages, or “necrotic” core areas did not differ significantly between groups. However, $ATM^{+/-}$ mice plaques had reduced apoptosis (Table).

To determine whether the increased atherosclerosis was mediated through ATM loss from circulating or vessel wall cells, we performed $ATM^{+/+}/ApoE^{-/-}$ bone marrow transplant (BMT) into irradiated $ATM^{+/-}/ApoE^{-/-}$ or $ATM^{+/+}/ApoE^{-/-}$ mice and fat fed them from 6 to 20 weeks. $ATM^{+/+}$ BMT completely (aorta) or partially (aortic root) rescued the accelerated atherosclerosis in $ATM^{+/-}/ApoE^{-/-}$ mice, such that plaque area differences in either vascular bed were not statistically significant (Figure 1C and 1D; Table). Plaque composition showed no significant changes in relative proportion of the major cell types. $ATM^{+/-}$ mice receiving $ATM^{+/+}$ BMT had increased cell proliferation yet retained reduced apoptosis (Table).

$ATM^{+/-}$ Mice Show Hyperlipidemia Before High-Fat Feeding

To examine how ATM heterozygosity promotes atherosclerosis, we examined lipid levels in mice before and after 14 weeks of fat feeding. $ATM^{+/-}/ApoE^{-/-}$ mice showed increased serum cholesterol, triglycerides and low-density lipoprotein cholesterol on both chow (Figure 2A) and fat feeding (Figure 2B). This hyperlipidemic profile was not corrected by $ATM^{+/+}$ BMT in mice on chow (Figure 2C), although serum cholesterol and triglyceride levels were not statistically different between genotypes after fat feeding of transplanted mice (Figure 2D).

$ATM^{+/-}/ApoE^{-/-}$ Mice Develop Multiple Features of the Metabolic Syndrome

The partial rescue of accelerated atherosclerosis in $ATM^{+/-}/ApoE^{-/-}$ mice after $ATM^{+/+}$ BMT suggests that ATM heterozygosity has direct effects on cells comprising the atherosclerotic plaque; however, BMT did not correct dyslipidemia seen in $ATM^{+/-}/ApoE^{-/-}$ mice, suggesting that ATM may regulate proatherosclerotic factors outside the vessel wall. Previous studies have shown that ATM deficiency results in elevated plasma apoB-48 levels with slower clearance of apoB-48–carrying lipoproteins[15] and affects the ability to complex with β-adaptin to promote endocytosis and accumulation of cytoplasmic lipid cytosomes,[23] along with several other features of the metabolic syndrome.[14]

Before fat feeding, 6-week-old $ATM^{+/-}/ApoE^{-/-}$ and $ATM^{+/+}/ApoE^{-/-}$ littermate controls had identical weights. However, after 14 weeks of fat feeding, ATM heterozygous mice were heavier (Figure 3A) and hypertensive (systolic average 98 mm Hg versus 115 mm Hg; Online Figure I). Visceral fat pads showed increased mean adipose weight (Figure 3B) and white adipose tissue demonstrated increased total adipocyte number (Figure 3C, upper images) and increased average cross sectional area (data not shown), with infiltration with mac-3 positive macrophages (data not shown). Similarly, livers from $ATM^{+/-}/ApoE^{-/-}$ mice showed extensive fat accumulation (Figure 3C, lower images), infiltration with inflammatory macrophages and neutrophils indicative of nonalcoholic steatohepatitis, and elevated liver serum transaminases and alkaline phosphatase (Figure 3D).

After fat feeding, $ATM^{+/-}/ApoE^{-/-}$ and $ATM^{+/+}/ApoE^{-/-}$ mice showed no differences in fasting glucose (data not shown) or HbA1C levels (Online Figure II). However, glucose tolerance of $ATM^{+/-}/ApoE^{-/-}$ mice was impaired compared to $ATM^{+/+}/ApoE^{-/-}$ mice after 7 weeks of fat feeding (Figure 3E). There was no difference in serum insulin or C-peptide (data not shown), suggesting possible differences in glucose sensing. Fasting insulin levels did increase over the experimental period but not between genotypes (data not shown), whereas insulin tolerance was unchanged (Figure 3F).

ATM Haploinsufficiency Induces DNA Damage in Cells Comprising Atherosclerotic Plaques

ATM deficiency or haploinsufficiency can cause failure to repair DNA and p53 activation, resulting in reduced apoptosis and growth arrest. We therefore examined cultured primary

VSMCs and macrophages derived from $ATM^{+/-}$ or $ATM^{+/+}$ mice for DNA damage, cell proliferation, and apoptosis. $ATM^{+/-}$ VSMCs and macrophages both showed increased micronuclei, an established marker of genomic instability (Figure 4A and Online Figure III). We have previously shown that the prooxidant t-BHP generates oxidative DNA damage in vascular cells, measured by comet assay.[10] $ATM^{+/-}$ VSMCs showed increased basal DNA fragmentation compared to $ATM^{+/+}$ VSMCs (Figure 4B), suggestive of impaired DNA repair. $ATM^{+/-}$ VSMCs had increased rates of proliferation both basally and after t-BHP (Figure 4C) and reduced rates of apoptosis (Figure 4D). Whereas terminally differentiated macrophages showed little proliferation (data not shown), apoptosis of $ATM^{+/-}$ macrophages was not different basally to $ATM^{+/+}$ macrophages but increased in response to t-BHP (Figure 4D). Accumulation of acetylated LDL in macrophages did not differ between genotypes (data not shown).

DNA damage activates ATM causing dimer disassociation, autophosphorylation and phosphorylation of downstream targets such as H2AX and p53. Phospho-ATM and γ-H2AX also bind to DNA breaks and are visible as macromolecular foci in cell nuclei. Indeed, $ATM^{+/-}$ VSMCs showed increased phospho-ATM and γ-H2AX foci compared to $ATM^{+/+}$ VSMCs (Figure 4E), consistent with persistent DNA damage and failure to repair DNA. To determine activation kinetics of DNA repair, we examined activation of ATM and its downstream substrates (γ-H2AX, Chk1 and Chk2 kinases and the key p53 residues ser15 and ser20). $ATM^{+/-}$ VSMCs had increased γ-H2AX activation both basally and after t-BHP treatment, with delayed activation of Chk-2, $p53^{ser15}$ and $p53^{ser20}$ but not Chk 1 (Figure 4F), consistent with basal DNA damage (and thus γ-H2AX phosphorylation), but defective p53 activation. In contrast, $ATM^{+/-}$ macrophages examined at the point of maximum DNA damage (on micronuclei assay) had impaired H2AX and ^{ser20}p53 phosphorylation but intact Chk1 and ^{ser15}p53 (Figure 4F), suggesting cell-specific defects in downstream signaling.

$ATM^{+/-}/ApoE^{-/-}$ Mice Have Disordered Metabolic Pathways in Multiple Metabolically Relevant Organs

The multiple metabolic syndrome features in $ATM^{+/-}/ApoE^{-/-}$ mice suggest that they have abnormal glucose and lipid metabolism. We therefore undertook metabolomic screening on tissue extracts from liver, pancreas, white adipose tissue and plasma using high-resolution ^{1}H-NMR spectroscopy (aqueous extracts), or gas chromatography (organic fraction). Datasets were analyzed using partial least squares–discriminant analysis to identify major metabolic differences between groups. $ATM^{+/-}/ApoE^{-/-}$ mice livers had increased β-hydroxybutyrate concentrations, but reduced lactate (Figure 5A, top) and glucose (Figure 5A, bottom). Plasma and pancreas of $ATM^{+/-}/ApoE^{-/-}$ mice showed a similar increase in β-hydroxybutyrate (Figure 5B). $ATM^{+/-}ApoE^{-/-}$ mice had significant differences in liver and pancreas fatty acid content with decreased oleic acid content and increases in other lipid moieties, including palmitic acid, linoleic acid, arachidonic acid and *cis*-4,7,10,13,16,19-docosahexaenoic acid (C22:6n3) (Figure 5C).

Effect of ATM on MtDNA and Function

Collectively, our metabolomic analysis suggested defects in respiratory chain function and lipid metabolism in $ATM^{+/-}/ApoE^{-/-}$ mice. As mitochondria generate ATP through oxidative phosphorylation, and their DNA is particularly sensitive to free radicals generated during this process, we examined total ROS production in vitro, mitochondrial content and MtDNA damage in $ATM^{+/+}$ and $ATM^{+/-}$ cells. Total cytosolic ROS production was significantly increased in age-matched $ATM^{+/-}/ApoE^{-/-}$ versus $ATM^{+/+}/ApoE^{-/-}$ VSMCs (Figure 6A), despite reduced total mitochondrial content as measured by citrate synthase activity (Online Figure IV).

MtDNA damage was assayed by identifying oxidative DNA adducts and a specific DNA deletion. Oxidative damage can introduce adducts into MtDNA that can block polymerase progression during PCR, reducing product abundance. By controlling cycle number to remain in the linear amplification phase, the amount of product produced is relative to the amount of MtDNA damage. We used a long 10-kb MtDNA target covering 60% of the mitochondrial genome to assess oxidative damage, compared to a short 127-bp target used to control for MtDNA copy number. Using this semiquantitative assay, global MtDNA damage from mice at 20 weeks of age was increased in $ATM^{+/-}$ mouse livers but not heart (Figure 6B).

The 4977-bp MtDNA common deletion is frequently observed in human atherosclerosis[1] and other diseases associated with aging. The complete 16-kb mitochondrial genome encodes 37 genes[24]; deletion of 4977 bp from nucleotide positions 8470 to 13447 bp spans 5 tRNA genes and 7 genes encoding mitochondrial respiratory chain polypeptides: ATP synthase subunit 6 (complex V), cyto-chrome *c* oxidase (complex IV), 4 polypeptides of NADH coenzyme Q reductase (complex I) (ND3, ND4, ND4L, and ND5), and 5 small tRNA.[25] The respiratory complexes are composed of nuclear and mitochondria-encoded polypeptides. For example complex I is composed of 45 polypeptides; only 7 are mitochondria-encoded but 5 of these are lost by the presence of the 4977-bp deletion. There are a variety of MtDNA deletions in mice, including 5-kb deletions equivalent to the human common deletion.[26],[27] We used a specific quantitative PCR–based assay that compared the amplification of a control sequence present in all mitochondria with the mutated sequence produced by the equivalent 4977-bp fragment excision. Absolute DNA quantification was performed using the comparative Ct method (Online Figure V).[28] Multiple tissues from $ATM^{+/-}$/ApoE and $ATM^{+/+}$/$ApoE^{-/-}$ mice were compared after 14 weeks of fat feeding. Although the fraction of heteroplasmy was small (<0.5% of MtDNA was the mouse equivalent of the human common MtDNA deleted form) (Figure 6C), $ATM^{+/-}$/ApoE mice showed increased levels of the deletion in multiple tissues, including, pancreas, liver, kidney, and skeletal muscle, but not brown and white adipose tissue or heart (Figure 6D).

To evaluate whether MtDNA damage correlated with changes in activity or expression of mitochondrial respiratory complexes, we assayed the respiratory complex subunit protein expression and activity in tissues with increased (liver) or similar (heart) levels of the MtDNA damage. Mitochondrial complex I to V expression was similar in $ATM^{+/+}$ and $ATM^{+/-}$ mouse livers (Figure 6E) and heart (data not shown), normalized either to the nuclear-encoded mitochondrial protein MnSOD or total mitochondrial protein (Online Figure VI). In contrast, using NADH-Ubiquinone Oxidoreductase assays, complex I activity was significantly reduced in $ATM^{+/-}$ versus $ATM^{+/+}$ mouse liver extracts when normalized to citrate synthase (Figure 6F) but not in heart (Online Figure VII). Citrate synthase normalized to mitochondrial protein was similar in $ATM^{+/+}$ and $ATM^{+/-}$ mouse livers (Online Figure VIII).

Discussion

Atherosclerosis is associated with DNA damage. DNA damage increases as atherosclerosis progresses and is present in both cells comprising plaques and peripheral blood cells. This widespread occurrence suggests that factors that promote DNA damage are attributable, at least in part, to systemic stimuli, such as risk factors that promote atherosclerosis. DNA damage is also determined by the capacity of cells that comprise the plaque to regulate DNA repair. DNA damage has profound effects on cell behavior; cell death, growth arrest, and cell senescence are all present in atherogenesis and contribute to acute effects such as plaque rupture and myocardial infarction. We have studied a model of widespread DNA damage,

that of systemic ATM haploinsufficiency, in atherosclerosis development and associated metabolic changes.

ATM haploinsufficiency promoted atherosclerosis in two separate vascular beds without changing plaque composition, indicating direct effects on multiple cell types that comprise the plaque and/or systemic risk factors. $ATM^{+/-}$ VSMCs and macrophages showed extensive genomic instability as indicated by micronucleus formation, nuclear DNA damage foci and DNA strand breaks. ATM haploinsufficiency had differing effects on cell proliferation and apoptosis of VSMCs and macrophages. $ATM^{+/-}$ VSMCs showed increased proliferation and reduced apoptosis, consistent with changes in downstream signaling pathways and the known role for ATM in regulating cell cycle arrest and apoptosis induced by DNA damage in dividing cells. Apoptosis was reduced in vivo in $ATM^{+/-}/ApoE^{-/-}$ mice plaques both with and without $ATM^{+/+}/ApoE^{-/-}$ BMT, suggesting that this may be attributable to reduced VSMC apoptosis in vivo. In contrast, $ATM^{+/-}$ macrophages showed increased apoptosis after oxidant stress. Both $ATM^{+/-}$ VSMCs and macrophages showed delayed signaling downstream from ATM (chk2, p53) which might partially account for these properties, although the differing sensitivities to apoptosis may be caused by different levels of sustained DNA damage and repair capacity, indicated by different relative γ-H2AX levels in $ATM^{+/+}$ and $ATM^{+/-}$ VSMCs and macrophages. Accelerated atherosclerosis was wholly (aorta) or partially (aortic root) corrected by BMT of $ATM^{+/+}$ cells, confirming a direct protective effect of ATM in atherogenesis. However, ATM haploinsufficiency promoted multiple features of the metabolic syndrome, including diet-induced obesity, preferential deposition of visceral fat, steatohepatitis, hypertension, hyperlipidemia, and glucose intolerance, that were not corrected by $ATM^{+/+}$ BMT.

To understand the profound changes in $ATM^{+/-}/ApoE^{-/-}$ mice, we profiled tissues that may contribute to the metabolic syndrome (white adipose tissues), pancreas, liver and plasma) using metabolomics. Metabolomics provides a snapshot of metabolic pathways and regulatory processes, reflecting the ultimate changes in a biological system after genetic and environmental influences.[29] $ATM^{+/-}/ApoE^{-/-}$ mice showed increased levels of β-hydroxybutyrate, a ketone body produced in the liver from incomplete oxidation of long chain fatty acids,[30] particularly when glucose cannot be effectively metabolized, for example in diabetes or when oxidative phosphorylation is compromised. The liver and pancreas of $ATM^{+/-}/ApoE^{-/-}$ mice also showed major lipid differences, including linoleic, oleic, palmitic and arachidonic acids, although the observed abnormal triglyceride and cholesterol accumulation may be a cause or consequence of other defects in lipid metabolism. For example, $ATM^{+/-}/ApoE^{-/-}$ mice have slower plasma apoB-48-carrying lipoprotein clearance,[15] and $ATM^{+/-}$ macrophages have increased macrophage lipoprotein lipase activity.[14]

We find evidence of MtDNA damage and dysfunction in $ATM^{+/-}$ cells and tissues. $ATM^{+/-}$ VSMCs showed increased ROS production despite reduced mitochondrial content, total MtDNA adducts were increased, and multiple tissues from $ATM^{+/-}$ mice showed increased levels of a mouse equivalent of the human common mitochondrial deletion, a region that encodes 7 genes for proteins comprising complexes I, IV, and V, indicating mitochondrial damage. Despite normal levels of complex subunit expression, $ATM^{+/-}$ mice livers had significantly reduced complex I activity compared with $ATM^{+/+}$ mice.

Our data are consistent with the following model (Figure 7). ATM heterozygosity promotes nuclear and MtDNA damage. Persistent DNA damage in plaque cells changes rates of cell proliferation and cell death that might directly promote atherosclerosis. ATM heterozygosity also promotes mitochondrial dysfunction, most likely attributable to a combination of increased ROS, MtDNA damage (eg, oxidative, or reduced nuclear-encoded mitochondrial

genes), and the MtDNA deletion, which leads to reduced complex I activity, reduced oxidative phosphorylation and further increased ROS and mitochondrial dysfunction. β-Oxidation of lipids under conditions of high-fat feeding promotes acetyl-coenzyme A accumulation and consequent production of acetoacetate. In $ATM^{+/-}/ApoE^{-/-}$ mice, elevated mitochondrial NADH reduces acetoacetate to β-hydroxybutyrate, which then accumulates. Although high cytosolic NADH would tend to increase lactate (a common finding in mitochondrial disease), the elevated mitochondrial acetyl-coenzyme A and NADH may occur simultaneously, which lowers glycolysis and reduces pyruvate availability to the mitochondria. This explanation is supported by findings of increased hepatic concentrations of *cis*-4,7,10,13,16,19-docosahexaenoic acid (DHA) (C22:6n3) in $ATM^{+/-}ApoE^{-/-}$ mice; DHA is a –3 polyunsaturated fatty acid that promotes fatty acid oxidation but suppresses glycolysis.[31] The combination of reduced glycolysis and abnormal lipid metabolism promotes lipid accumulation and glucose intolerance, promoting atherosclerosis and leading to features of the metabolic syndrome.

Although this model can explain most of our findings, we have not directly proven the link between reduced oxidative phosphorylation and glucose intolerance and abnormal lipid metabolism in $ATM^{+/-}/ApoE^{-/-}$ mice. Complete ATM loss also results in tissue-specific alterations in MtDNA copy number and reduced function of ribonucleotide reductase, the rate-limiting enzyme in de novo synthesis of deoxyribonucleoside triphosphates, potentially linking genomic instability in $ATM^{-/-}$ cells with a similar mitochondria-deficient phenotype.[16] Our data also do not prove that the MtDNA dysfunction is attributable to increased ROS production or MtDNA damage or the deletion alone. Nuclear DNA damage, as evidenced here by DNA damage foci, DSBs, and reduced repair capacity, can also promote mitochondrial dysfunction and MtDNA damage. In humans, there are at least 813 nuclear gene transcripts and proteins that relate to mitochondrial function and homeostasis[32]; nuclear DNA damage may therefore also disrupt MtDNA copy number and function directly.

In summary, we demonstrate that ATM haploinsufficiency promotes atherosclerosis, via both direct effects on vessel wall cells and multiple systemic proatherosclerotic features of the metabolic syndrome. MtDNA damage, increased ROS, and reduced oxidative phosphorylation may link defects in DNA repair and changes in glucose and lipid metabolism.

Novelty and Significance

What Is Known?

- DNA damage, including mitochondrial DNA damage, has been detected in atherosclerotic lesions.
- Haploinsufficiency of the DNA repair protein ATM (ataxia telangiectasia mutated) promotes atherosclerosis and features of the metabolic syndrome. The mechanism underlying these effects is not fully known.

What New Information Does This Article Contribute?

- ATM haploinsufficiency promotes atherosclerosis via direct effects on cells that comprise the plaque (vascular smooth muscle cells and macrophages) and by promoting multiple features of the metabolic syndrome.
- ATM haploinsufficiency promotes mitochondrial DNA damage and reduced function.

- Mitochondrial dysfunction within metabolically active tissues may promote the metabolic syndrome.

DNA damage is associated with atherosclerosis, but it is not known whether this association is causal, and, if so, what the underlying mechanism(s) is. We used 50% loss of the DNA repair protein ATM to model how DNA damage could promote atherosclerosis in ApoE-null mice. ATM haploinsufficiency increased atherosclerosis, that was partly inhibited by bone marrow transplant of $ATM^{+/+}$ cells. ATM haploinsufficiency increased reactive oxygen species, caused nuclear and mitochondrial DNA damage, and altered cell death and cell proliferation in smooth muscle cells and macrophages, suggesting a direct effect on cells comprising plaques. However, ATM haploinsufficiency also promoted mitochondrial DNA damage in multiple tissues and respiratory chain dysfunction in liver tissue. Lipid and glucose metabolic defects in $ATM^{+/-}$ mice caused multiple features of the metabolic syndrome, also promoting atherosclerosis through systemic effects. This work identifies DNA damage and mitochondrial dysfunction as key links between atherosclerosis and the metabolic syndrome. Our work suggests that DNA damage potentially plays a causal role in atherogenesis, via both direct and systemic actions. Reducing DNA damage and increasing mitochondrial function may represent new therapeutic targets to inhibit both atherosclerosis and the metabolic syndrome.

Supplementary Material

Refer to Web version on PubMed Central for supplementary material.

Acknowledgments

We acknowledge the help of Tracy Prime and Irina Abakumova with mitochondrial extraction and respiratory complex activity assays.

Sources of Funding

This work was supported by British Heart Foundation (BHF) grant RG08/009/25841 (to M.B.); Diabetes and Wellness Foundation, Biotechnology and Biological Sciences Research Council (BBSRC), British Heart Foundation (PG/05/08), and Wellcome Trust (072829/ Z/03/Z) grants (to J.G.); Medical Research Council (MRC) and Hepadip grants (to A.V.-P.); the European Vascular Genomics Network; and the Cambridge National Institute for Health Research (NIHR) Biomedical Research Centre.

Non-standard Abbreviations and Acronyms

ApoE	apolipoprotein E
ATM	ataxia telangiectasia mutated
BMT	bone marrow transplant
DSB	double-stranded break
H2AX	histone 2A gene
HbA1c	glycosylated hemoglobin
MtDNA	mitochondrial DNA
MnSOD	manganese superoxide dismutase
ROS	reactive oxygen species
SMA	smooth muscle cell actin

Europe PMC Funders Author Manuscripts

VSMC vascular smooth muscle cell

References

1. Botto N, Rizza A, Colombo MG, Mazzone AM, Manfredi S, Masetti S, Clerico A, Biagini A, Andreassi MG. Evidence for DNA damage in patients with coronary artery disease. Mutat Res. 2001; 493:23–30. [PubMed: 11516712]
2. Andreassi M, Botto N. DNA damage as a new emerging risk factor in atherosclerosis. Trends Cardiovasc Med. 2003; 13:270–275. [PubMed: 14522466]
3. Groemping Y, Rittinger K. Activation and assembly of the NADPH oxidase: a structural perspective. Biochem J. 2005; 386:401–416. [PubMed: 15588255]
4. Ballinger SW. Mitochondrial dysfunction in cardiovascular disease. Free Radic Biol Med. 2005; 38:1278–1295. [PubMed: 15855047]
5. Gorenne I, Kavurma M, Scott S, Bennett M. Vascular smooth muscle cell senescence in atherosclerosis. Cardiovasc Res. 2006; 72:9–17. [PubMed: 16824498]
6. Martinet W, Knaapen MW, De Meyer GR, Herman AG, Kockx MM. Elevated levels of oxidative DNA damage and DNA repair enzymes in human atherosclerotic plaques. Circulation. 2002; 106:927–932. [PubMed: 12186795]
7. Puddu GM, Cravero E, Arnone G, Muscari A, Puddu P. Molecular aspects of atherogenesis: new insights and unsolved questions. J Biomed Sci. 2005; 12:839–853. [PubMed: 16328782]
8. Lee JW, Kusumoto R, Doherty KM, Lin GX, Zeng W, Cheng WH, von Kobbe C, Brosh RM Jr, Hu JS, Bohr VA. Modulation of Werner syndrome protein function by a single mutation in the conserved RecQ domain. J Biol Chem. 2005; 280:39627–39636. [PubMed: 16150736]
9. Matthews C, Gorenne I, Scott S, Figg N, Kirkpatrick P, Ritchie A, Goddard M, Bennett M. Vascular smooth muscle cells undergo telomere-based senescence in human atherosclerosis: effects of telomerase and oxidative stress. Circ Res. 2006; 99:156–164. [PubMed: 16794190]
10. Mahmoudi M, Gorenne I, Mercer J, Figg N, Littlewood T, Bennett M. Statins use a novel Nijmegen breakage syndrome-1-dependent pathway to accelerate DNA repair in vascular smooth muscle cells. Circ Res. 2008; 103:717–725. [PubMed: 18723444]
11. Ballinger S, Patterson C, Yan C, Doan R, Burow D, Young C, Yakes F, van Houten B, Ballinger C, Freeman B, Runge M. Hydrogen peroxide and peroxynitrite induced mitochondrial DNA damage and dysfunction in vascular endothelial and smooth muscle cells. Circ Res. 2000; 86:960–966. [PubMed: 10807868]
12. Croteau DL, Stierum RH, Bohr VA. Mitochondrial DNA repair pathways. Mutat Res. 1999; 434:137–148. [PubMed: 10486588]
13. Ballinger SW, Patterson C, Knight-Lozano CA, Burow DL, Conklin CA, Hu Z, Reuf J, Horaist C, Lebovitz R, Hunter GC, McIntyre K, Runge MS. Mitochondrial integrity and function in atherogenesis. Circulation. 2002; 106:544–549. [PubMed: 12147534]
14. Schneider JG, Finck BN, Ren J, Standley KN, Takagi M, Maclean KH, Bernal-Mizrachi C, Muslin AJ, Kastan MB, Semenkovich CF. ATM-dependent suppression of stress signaling reduces vascular disease in metabolic syndrome. Cell Metab. 2006; 4:377–389. [PubMed: 17084711]
15. Wu D, Yang H, Xiang W, Zhou L, Shi M, Julies G, Laplante JM, Ballard BR, Guo Z. Heterozygous mutation of ataxia-telangiectasia mutated gene aggravates hypercholesterolemia in apoE-deficient mice. J Lipid Res. 2005; 46:1380–1387. [PubMed: 15863839]
16. Eaton JS, Lin ZP, Sartorelli AC, Bonawitz ND, Shadel GS. Ataxiatelangiectasia mutated kinase regulates ribonucleotide reductase and mitochondrial homeostasis. J Clin Invest. 2007; 117:2723–2734. [PubMed: 17786248]
17. Ambrose M, Goldstine JV, Gatti RA. Intrinsic mitochondrial dysfunction in ATM-deficient lymphoblastoid cells. Hum Mol Genet. 2007; 16:2154–2164. [PubMed: 17606465]
18. Miles PD, Treuner K, Latronica M, Olefsky JM, Barlow C. Impaired insulin secretion in a mouse model of ataxia telangiectasia. Am J Physiol Endocrinol Metab. 2007; 293:E70–E74. [PubMed: 17356010]

19. Mercer J, Figg N, Stoneman V, Braganza D, Bennett MR. Endogenous p53 protects vascular smooth muscle cells from apoptosis and reduces atherosclerosis in ApoE knockout mice. Circ Res. 2005; 96:667–674. [PubMed: 15746445]
20. Stoneman V, Braganza D, Figg N, Mercer J, Lang R, Goddard M, Bennett M. Monocyte/macrophage suppression in CD11b diphtheria toxin receptor transgenic mice differentially affects atherogenesis and established plaques. Circ Res. 2007; 100:884–893. [PubMed: 17322176]
21. Kirsch-Volders M, Elhajouji A, Cundari E, Van Hummelen P. The in vitro micronucleus test: a multi-endpoint assay to detect simultaneously mitotic delay, apoptosis, chromosome breakage, chromosome loss and non-disjunction. Mutat Res. 1997; 392:19–30. [PubMed: 9269328]
22. Ostling O, Johanson KJ. Microelectrophoretic study of radiation-induced DNA damages in individual mammalian cells. Biochem Biophys Res Commun. 1984; 123:291–298. [PubMed: 6477583]
23. Lim DS, Kirsch DG, Canman CE, Ahn JH, Ziv Y, Newman LS, Darnell RB, Shiloh Y, Kastan MB. ATM binds to beta-adaptin in cytoplasmic vesicles. Proc Natl Acad Sci U S A. 1998; 95:10146–10151. [PubMed: 9707615]
24. Andrews RM, Kubacka I, Chinnery PF, Lightowlers RN, Turnbull DM, Howell N. Reanalysis and revision of the Cambridge reference sequence for human mitochondrial DNA. Nat Genet. 1999; 23:147. [PubMed: 10508508]
25. Dani MA, Dani SU, Lima SP, Martinez A, Rossi BM, Soares F, Zago MA, Simpson AJ. Less DeltamtDNA4977 than normal in various types of tumors suggests that cancer cells are essentially free of this mutation. Genet Mol Res. 2004; 3:395–409. [PubMed: 15614730]
26. Muscari C, Giaccari A, Stefanelli C, Viticchi C, Giordano E, Guarnieri C, Caldarera CM. Presence of a DNA-4236 bp deletion and 8-hydroxy-deoxyguanosine in mouse cardiac mitochondrial DNA during aging. Aging (Milano). 1996; 8:429–433. [PubMed: 9061131]
27. Srivastava S, Moraes CT. Double-strand breaks of mouse muscle mtDNA promote large deletions similar to multiple mtDNA deletions in humans. Hum Mol Genet. 2005; 14:893–902. [PubMed: 15703189]
28. Schmittgen TD, Livak KJ. Analyzing real-time PCR data by the comparative C(T) method. Nat Protoc. 2008; 3:1101–1108. [PubMed: 18546601]
29. Fiehn O. Metabolomics-the link between genotypes and phenotypes. Plant Mol Biol. 2002; 48:155–171. [PubMed: 11860207]
30. McGarry JD, Foster DW. Regulation of hepatic fatty acid oxidation and ketone body production. Annu Rev Biochem. 1980; 49:395–420. [PubMed: 6157353]
31. Jump DB, Botolin D, Wang Y, Xu J, Demeure O, Christian B. Docosahexaenoic acid (DHA) and hepatic gene transcription. Chem Phys Lipids. 2008; 153:3–13. [PubMed: 18343222]
32. Catalano D, Licciulli F, Turi A, Grillo G, Saccone C, D'Elia D. MitoRes: a resource of nuclear-encoded mitochondrial genes and their products in Metazoa. BMC Bioinformatics. 2006; 7:36. [PubMed: 16433928]

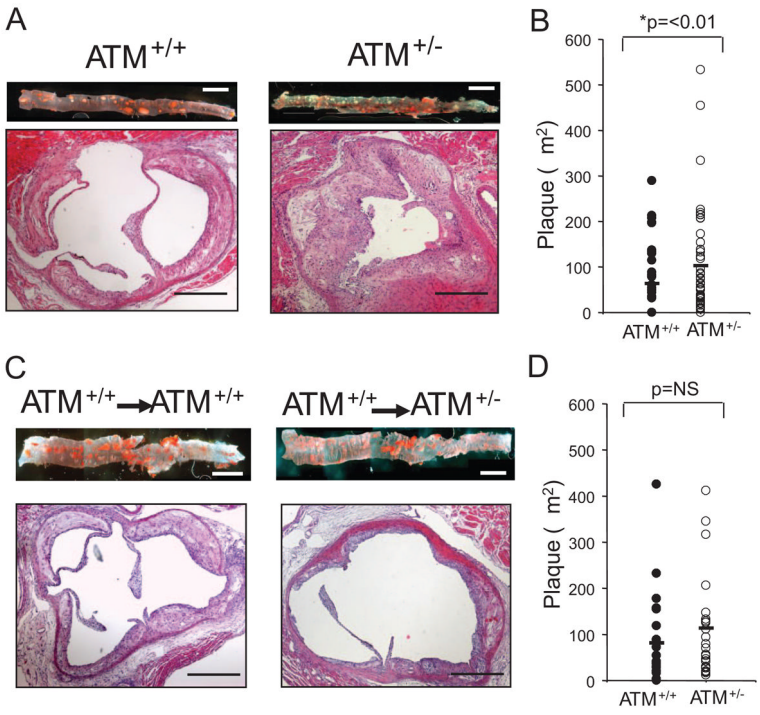

Figure 1. ATM$^{+/-}$/ApoE$^{-/-}$ mice have accelerated atherosclerosis.

A, Comparison of atherosclerotic lesions from ATM$^{+/+}$/ApoE$^{-/-}$ (n=13) and ATM$^{+/-}$/ApoE$^{-/-}$ mice (n=15). Descending aorta was stained for neutral lipid with oil red O (upper images). **Scale bar** is 1 mm. **Lower images** show aortic root section stained with H+E. **Scale bars** are 500 μm. **B,** Histogram of aortic root plaque area in ATM$^{+/+}$/ApoE$^{-/-}$ and ATM$^{+/-}$/ApoE$^{-/-}$ mice. **C,** Descending aorta **(upper images)** and aortic root sections **(lower images)** from ATM$^{+/+}$/ApoE$^{-/-}$ (n=7) or ATM$^{+/-}$/ApoE$^{-/-}$ mice (n=8), after ATM$^{+/+}$/ApoE$^{-/-}$ BMT. **D,** Histogram of aortic root plaque area in transplanted mice.

Europe PMC Funders Author Manuscripts

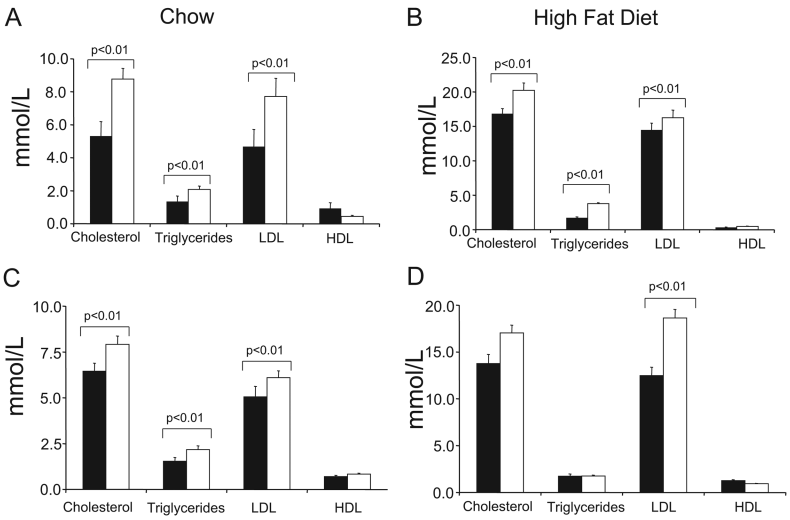

Figure 2. ATM$^{+/-}$/ApoE$^{-/-}$ mice show hyperlipidemia

A and B, Serum lipids in ATM$^{+/+}$/ApoE$^{-/-}$ **(black bars)** (n=13) or ATM$^{+/-}$/ApoE$^{-/-}$ **(open bars)** (n=15) mice fed either normal chow **(A)** or after 14 weeks of fat feeding (**B**). **C and D,** Serum lipids in ATM$^{+/+}$/ApoE$^{-/-}$ or ATM$^{+/-}$/ApoE$^{-/-}$ mice receiving ATM$^{+/+}$/ApoE$^{-/-}$ BMT, fed either normal chow (n=7) **(C)** or after 14 weeks of fat feeding (n=8) **(D)**.

Europe PMC Funders Author Manuscripts

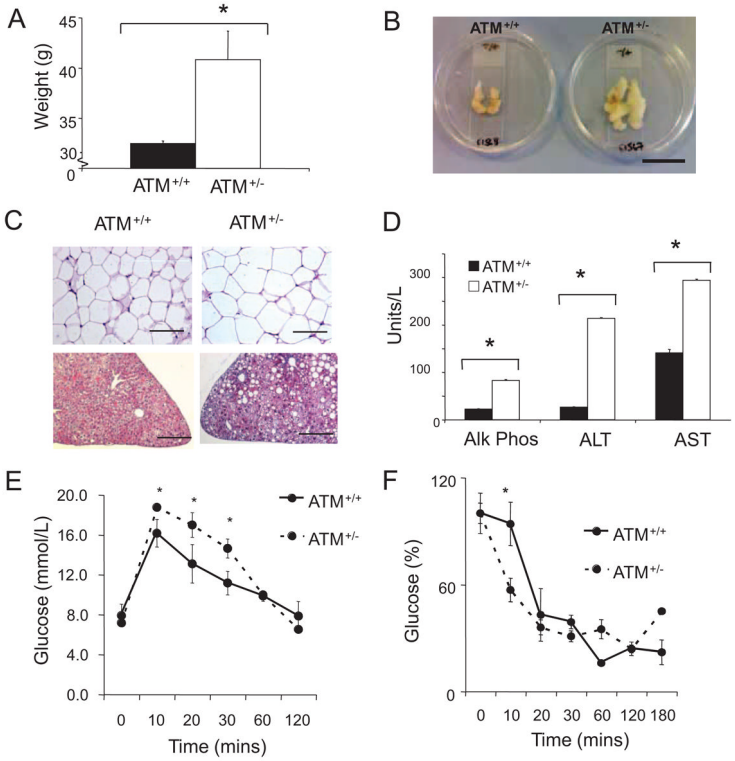

Figure 3. ATM$^{+/-}$/ApoE$^{-/-}$ mice show multiple features of the metabolic syndrome

A, Body weight for ATM$^{+/+}$/ApoE$^{-/-}$ (n=10) and ATM$^{+/-}$/ApoE$^{-/-}$ (n=6) mice after 14 weeks of high-fat feeding. **B,** Abdominal visceral fat pad from same experimental groups as in **A**. **Scale bar** is ≈4 cm. **C,** Representative (×20) images of white adipose tissue demonstrating adipocyte hypertrophy **(upper images)** and H and E-stained liver sections showing hepatic steatosis **(lower images). Scale bar** is 200 μm. **D,** Serum liver enzymes including alkaline phosphatase (AlkPhos), alanine transaminase (ALT), and aspartate transaminase (AST) in ATM$^{+/+}$/ApoE$^{-/-}$ mice and ATM$^{+/-}$/ApoE$^{-/-}$ mice. *P<0.001 (n=5). **E,** Fasted glucose tolerance test in ATM$^{+/+}$/ApoE$^{-/-}$ mice and ATM$^{+/-}$/ApoE$^{-/-}$ mice after 7 weeks of high-fat feeding (n=5). **F,** Insulin tolerance test in ATM$^{+/+}$/ApoE$^{-/-}$ mice and ATM$^{+/-}$/ApoE$^{-/-}$ mice after 7 weeks of high-fat feeding. All data are means; error bars represent SEMs. *P=<0.01 (n=5).

Europe PMC Funders Author Manuscripts

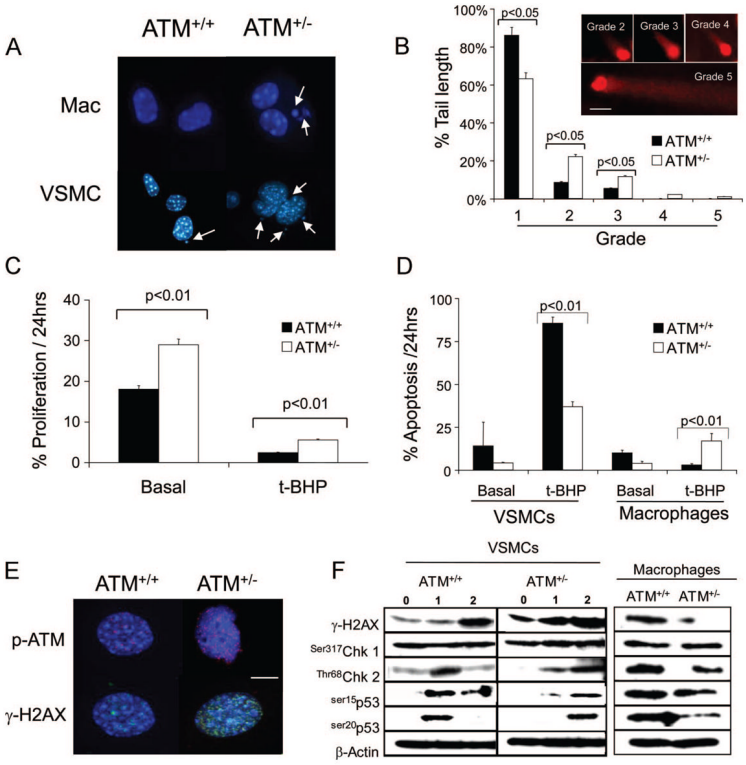

Figure 4. ATM$^{+/-}$ cells demonstrate genomic instability, abnormal cell proliferation, and apoptosis

A, Micronuclei in macrophages and VSMCs from ATM$^{+/+}$/ApoE$^{-/-}$ and ATM$^{+/-}$/ApoE$^{-/-}$ mice (n=3). **B,** Quantification of DNA comet tails lengths by grade (inset) in ATM$^{+/+}$/ApoE$^{-/-}$ and ATM$^{+/-}$/ApoE$^{-/-}$ VSMCs. Cells were incubated for 1 hour with 10 μmol/L t-BHP and comet tails estimated 1 hour later (scale bar=20 μm), n=3. **C and D,** Percentage of ATM$^{+/+}$/ApoE$^{-/-}$ and ATM$^{+/-}$/ApoE$^{-/-}$ VSMCs undergoing proliferation **(C)** or apoptosis in ATM$^{+/+}$/ApoE$^{-/-}$ and ATM$^{+/-}$/ApoE$^{-/-}$ VSMCs and macrophages **(D)** assessed by time-lapse videomicroscopy over 24 hours, both basally and after exposure to 10 μmol/L t-BHP (n=3). **E,** Immunocytochemistry of DNA damage foci expression of phospho-ATM **(red)** and γ-H2AX **(green)** in ATM$^{+/+}$/ApoE$^{-/-}$ and ATM$^{+/-}$/ApoE$^{-/-}$ VSMCs after 10 μmol/L t-BHP for 1 hour and 1-hour recovery. Nuclei are counterstained with DAPI **(blue)**. **Scale bar** is 20 μm. **F,** Western blot of ATM$^{+/+}$/ApoE$^{-/-}$ and ATM$^{+/-}$/ApoE$^{-/-}$ VSMCs basally (0 hour), after 1 hour of treatment with 10 μmol/L t-BHP (1 hour), and after 1 hour of recovery (2 hours) or ATM$^{+/+}$/ApoE$^{-/-}$ and ATM$^{+/-}$/ApoE$^{-/-}$ macrophages after 1 hour of treatment with 10 μmol/L t-BHP and 1 hour of recovery.

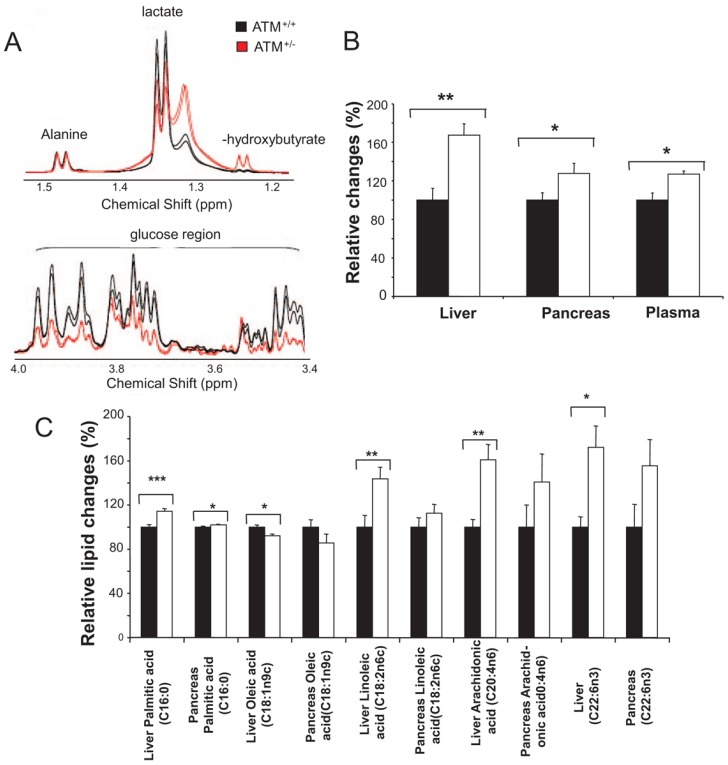

Figure 5. ATM$^{+/-}$ mice show a defect in oxidative phosphorylation on metabolomic screening

A, High-resolution 500 MHz ^{1}H-NMR spectra of liver extracts from ATM$^{+/+}$/ApoE$^{-/-}$ and ATM$^{+/-}$/ApoE$^{-/-}$ mice. **Top,** β-Hydroxybutyrate, lactate, and alanine peaks are labeled. **Bottom,** Multiple peaks show the glucose region in NMR spectra. **B,** β-Hydroxybutyrate concentrations in liver, pancreas, and plasma of ATM$^{+/-}$/ApoE$^{-/-}$ mice. Data are shown as relative changes in ATM$^{+/+}$/ApoE$^{-/-}$ compared with ATM$^{+/+}$/ApoE$^{-/-}$ mice (means±SEM). *P<0.05, **P<0.01. **C,** Major lipid changes in the liver and pancreas. Data are shown as relative changes in ATM$^{+/+}$/ApoE$^{-/-}$ compared with ATM$^{+/+}$/ApoE$^{-/-}$ mice (means±SEM). *P<0.05, **P<0.01, ***P<0.001. Black bars indicate ATM$^{+/+}$/ApoE$^{-/-}$; unfilled bars, ATM$^{+/-}$/ApoE$^{-/-}$.

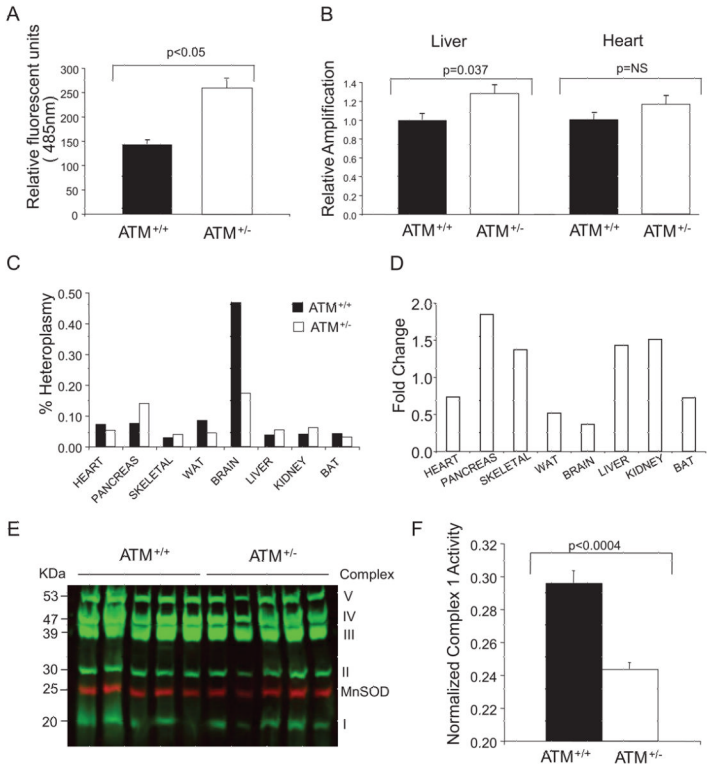

Figure 6. ATM$^{+/-}$ mitochondria have increased ROS production and MtDNA damage

A, ROS production assayed using the ROS-sensitive fluorochrome DCFDA in ATM$^{+/+}$ and ATM$^{+/-}$ VSMCs. **B,** MtDNA adducts determined by semiquantitative PCR. **C,** Degree of heteroplasmy in tissues from ATM$^{+/-}$/ApoE$^{-/-}$ and ATM$^{+/+}$/ApoE$^{-/-}$ mice after 14 weeks of high-fat feeding. **D,** Fold increase in mitochondrial common mutation in tissues from ATM$^{+/-}$/ApoE$^{-/-}$ relative to ATM$^{+/+}$/ApoE$^{-/-}$ mice. BAT indicates brown adipose tissue; WAT, white adipose tissue. **E,** Quantitative fluorescent Western blot of liver mitochondrial respiratory complex proteins relative to the nuclear-encoded mitochondrial protein MnSOD. **F,** Liver mitochondrial complex I respiratory activity normalized to the nuclear-encoded mitochondrial protein citrate synthase.

Europe PMC Funders Author Manuscripts

Europe PMC Funders Author Manuscripts

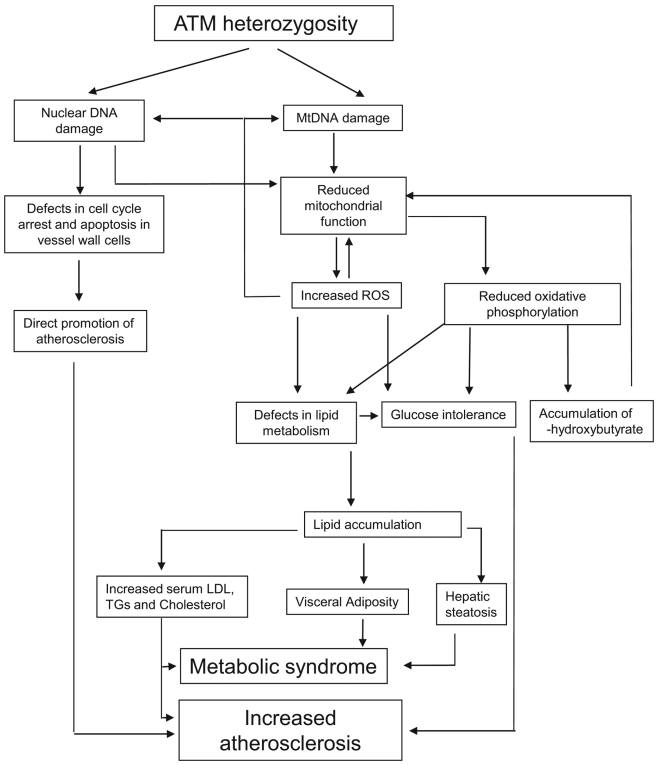

Figure 7.
Proposed model of increased atherosclerosis and metabolic syndrome in ATM$^{+/-}$/ApoE$^{-/-}$ mice.

Europe PMC Funders Author Manuscripts

Table

Atherosclerosis Is Increased in $ATM^{+/-}/ApoE^{-/-}$ Mice

			Bone Marrow Transplant	
	$ATM^{+/+}$ (n=13)	**$ATM^{+/-}$ (n=15)**	**$ATM^{+/+} \rightarrow ATM^{+/+}$ (n=7)**	**$ATM^{+/+} \rightarrow ATM^{+/-}$ (n=8)**
Aortic Plaque area (mm^2)	4.76±1.07	8.26±2.32 *	2.78±0.73	2.03±0.91
Aortic Root per Plaque area (μm^2)	63.93±12.9	103.14±17.4 *	81.94±22.5	114.17±22.4
SMA positive area (%)	5.68±1.72	4.23±0.83	13.92±6.94	11.9±2.92
MAC positive area (%)	39.81±3.53	32.42±4.63	46.47±10.14	58.66±6.99
Necrotic core area (%)	34.35±4.15	34.30±5.74	71.91±5.57	66.31±3.39
Ki67 positive cells (%)	0.68±0.10	0.29±0.1	0.89±0.20	2.15±0.55 *
Cleaved caspase 3–positive cells (%)	0.55±0.07	0.22±0.07 *	0.82±0.15	0.28±0.17 *

Left columns: atherosclerotic plaque areas, % SMA, Mac-3, and necrotic core areas, and percentage of cells undergoing cell proliferation (Ki67) or apoptosis (CC3) in $ATM^{+/+}/ApoE^{-/-}$ or $ATM^{+/-}/ApoE^{-/-}$ mice. Right columns: Plaque areas and percentages for $ATM^{+/+}/ApoE^{-/-}$ or $ATM^{+/-}/ApoE^{-/-}$ mice undergoing $ATM^{+/+}/ApoE^{-/-}$ BMT. Data are means±SEM.

* $P<0.05$ for $ATM^{+/-}$ mice vs $ATM^{+/+}$ mice, or $ATM^{+/-}$ vs $ATM^{+/+}$ recipients.